International Journal of GEOMATE, June., 2021, Vol.20, Issue 82, pp.170-185
ISSN: 2186-2982 (P), 2186-2990 (O), Japan, DOI: https://doi.org/10.21660/2021.82.j2114
Geotechnique, Construction Materials and Environment

GEOCHEMICAL INVESTIGATION ON JABOI MANIFESTATION, JABOI VOLCANO, SABANG, INDONESIA

*Rinaldi Idroes[1], Marwan Marwan[2], Muhammad Yusuf[1], Muslem Muslem[3], and Zuchra Helwani[4]

[1]Department of Chemistry, Faculty of Mathematics and Natural Sciences, Universitas Syiah Kuala, Indonesia
[2]Department of Geophysic Engineering, Faculty of Engineering, Universitas Syiah Kuala, Indonesia
[3]Department of Chemistry, Faculty of Science and Technology, Universitas Islam Negeri Ar-Raniry, Indonesia, [4]Department of Chemical Engineering, Faculty of Engineering, Universitas Riau, Indonesia

*Corresponding Author, Received: 13 Feb. 2021, Revised: 27 Feb. 2021, Accepted: 08 Mar. 2021

ABSTRACT: Geochemical studies have been conducted in the geothermal system of Jaboi manifestation, Sabang, Aceh. There are three sub-area of geothermal water sites in this area, that are production-injection wells of PT Sabang Geothermal Energy, Jaboi crater, and hot spring pond. The fumaroles were also found in the Jaboi crater. The mineral contents were analyzed by ion chromatography, alkalimetry, and spectrophotometry, the isotope was determined by Laser Absorption Spectrophotometer, while the gas contents were analyzed by Gas Chromatography-TCD. The obtained data were used to estimate the reservoir temperature by using geothermometers, FT-HSH diagram, and CH_4/CO_2-H_2/Ar diagram. The graphical analysis were also done to obtain chemical and physical characteristics. The water analysis showed that the reservoir temperatures were in range of 253.2-416.5 °C. The water types of production-injection wells, Jaboi crater and hot spring pond were chloride, sulphate and bicarbonate-sulphate mixtures, respectively. The fluid equilibria showed that only production well was mature water while the other sites were immature ones. The water composition source of production-injection wells and hot spring pond were marine sedimentary rocks, Jaboi crater JK1 and JK4 were magmatic gas, and Jaboi crater JK2 was hot rock. The water origin of production-injection wells were both magmatic and meteoric, Jaboi craters were magmatic water, and hot spring pond was meteoric water. The gas analysis in Jaboi crater fumaroles showed that the reservoir temperature were in range of 196.9-362.8 ºC, and the gas origin were earth's crust. The reservoir temperatures showed a high-temperature geothermal system which is suitable for power plant.

Keywords: Hydro-geothermometry, Gas-geothermometry, Isotope analysis, Jaboi sabang mountain, Indonesia

1. INTRODUCTION

Greenhouse gases, especially carbon dioxide released by burning fossil fuel, have caused the increase of atmosphere temperature [1]. To reduce this negative impact, the use of renewable energy sources is highly recommended [2]. Some countries have selected solar energy for electricity generation [3,4], but this resource is only available during sunny days and requires energy storage such as batteries [5-7]. Some tropical countries have successfully adopted biofuel [8-10], but the use of edible crops and the utilization of productive land for biofuel material make conflicts with food production. Due to this reason, Indonesia is attempting to develop geothermal energy as an alternative to fossil fuels.

Indonesia has 40% of the world's total geothermal potentials [11], but it is only 6.2% that has been exploited. To incentivize the geothermal electricity target, the Indonesian government has planned the 6,000 MWe in the short-medium term development program year 2025 [12], hence the exploration studies are urgent. There are at least three essential exploration data to determine the feasibility of geothermal exploitation to generate electricity, they are; geology, geophysics, and geochemistry [13–15]. Among those three, geochemistry holds an important role in the exploration of geothermal conditions, especially in the temperature estimation to determine the generatable energy capacity [16].

Geothermal exploitation for electricity in Indonesia is still concentrated in the Java island, but almost half of Indonesia's geothermal potential is located on the Sumatra island [12]. Aceh is a province in Sumatra with enormous geothermal potential. Based on the records, there are three geothermal potentials in Aceh, they are; Seulawah Agam, Jaboi, and Geuredong volcanoes. Even though the production has not been made, the publication pertaining to the exploration of Seulawah Agam volcano has indicated a significant development. Some geophysical studies have reported geothermal feature [17] and the deep and shallow data of the subsurface structure of the geothermal system [18]. Heat source locations had also been imaged by MT and TEM data [19]. Geochemical studies indicate that manifestation in the southern zone in particular Ie Seu'um [20], Ie Brouk [21], Ie Ju [22] and Van Heutz Crater, are high-temperature geothermal systems [23] that are

very suitable for electricity generation. Besides the temperature estimation, the research data also informed the water type, the chemical composition, the fluid equilibrium, and the fluid origins.

In contrast with Seulawah Agam, there is still little reported data on the exploration of the Jaboi volcano. There are almost no publications on the exploration data which are holistic and credible for energy purposes, especially the geochemical data. There are only geophysical data regarding the mapping of heat locations found [24]. As one of the outermost islands, a sufficient electricity supply is very needed. With an estimated capacity of 11.5 MWe [25], the Jaboi volcano is an essential resource to fulfill the electricity demand of the island that has a size of 153 Km^2, with tourism as its main economic support.

The three aspects; hydro-geochemistry, gas-geochemistry, and isotope analysis, have to be conducted simultaneously in every geochemical study. Apart from those three, to estimate the reservoir temperature, a geothermometer can be used instead, where the other important geochemical characteristics are determined by using graphical plots. The hydro-geochemical analysis gives the information on dominant chemical compositions, the type and equilibrium of geothermal water, while gas-geochemical analysis gives the information on the fumarole sources and the dominant fluid phases lastly, isotope analysis gives the information on the geothermal water origins [23,26].

The accuracy of the chemical measurement in the sample highly determines both the geothermometer calculation and the graphical plotting results. Therefore, the analytical method and instruments have to be accurate and reliable. The methods recommended for such purposes, some of them, are ICP-OES, UV-Vis Spectrophotometer [23,27], ICP-AES, ICP-MS [26] and Laser-Induced Breakdown Spectroscopy [28–30] for cation analysis, Ion Chromatography for either cation or anion analysis [31], Elemental Analyzer-Isotope Ratio Mass Spectrophotometry [32] and Laser Absorption Spectroscopy [33] for isotope analysis.

In this research, geochemical studies were conducted in Jaboi manifestation in the geothermal area of Jaboi volcano, Sabang. This research includes in-situ, geothermal water, geothermal gas, and isotopes analysis. Ions in the water and gas were analyzed by Ion Chromatography, Spectrophotometer Uv-Vis, and alkalimetry titration. Meanwhile, the isotope analysis was conducted by Laser Absorption Spectrophotometer. Several geothermometry namely hydro-Geothermometer, Gas-Geothermometer, and stable isotope plotting methods were applied to obtain the geochemical information, which includes the information of the water type, water chemical analysis, water equilibrium, predicted reservoir temperature and the origin of the geothermal fluids.

2. THE INVESTIGATED AREA

Jaboi volcano is located in Weh Island (also known as Sabang Island), the Northwest of Sumatra Island, Aceh Province, Indonesia. There are three geothermal manifestations in that location, they are: Iboih, Pria Laot, and Jaboi [34]. Jaboi manifestation is located around the border between Sukajaya and Sukakarya Sub-Districts.

The southwest Jaboi manifestation has been exploited by PT. Sabang Geothermal Energy since early 2017. This project is still in the construction phase to date. Two sampling points were established in this area, which is the production well and the injection well, denoted by SP1 and SP2, respectively. One sampling point, denoted by KP, was set in the northeastern of Jaboi manifestation. There is a hot spring in this area. Five sampling points were set in the middle of Jaboi manifestation around the Jaboi crater. There are three hot springs denoted by JK1, JK2, and JK4, and also two fumaroles denoted by KJ2 and KJ3. All mentioned sampling point locations can be seen in Fig 1. Geologically (Fig 2), Jaboi mountain has a volcanic formation Leumo Matee, with the stream Piroklastik Leumo Matee, the volcanic formation Seumeuruguh and the Prioklastik Seumeuruguh stream [35].

3. METHODS

3.1 Geothermal Water Samples and Sampling Methods

The initial step was a survey of the geothermal sources in Jaboi manifestation, Sabang. The water samples were collected from hot spring in sampling points around PT. Sabang Geothermal Energy area (SP1 and SP2), hot spring pond (KP), and Jaboi crater (JK1, JK2 and JK4). Coordinate and elevation data of each sampling point were marked with GPS (Garmin 62S). The samples were collected into polyethylene bottles (PE) and filtered with a Whatman 0.45 μm filter paper. For cation analysis, the samples were added with HNO_3 6 N until pH < 2 was reached (acidified), while for anion analysis, the samples were treated without HNO_3 addition (non-acidified). For SiO_2 analysis, the samples were diluted with deionized water to avoid silica precipitation. For isotope analysis (δD and $\delta^{18}O$), the samples were collected into bottle 50 mL. To maintain the samples' quality, the bottles were stored in a cool box and transported to the laboratory for analysis.

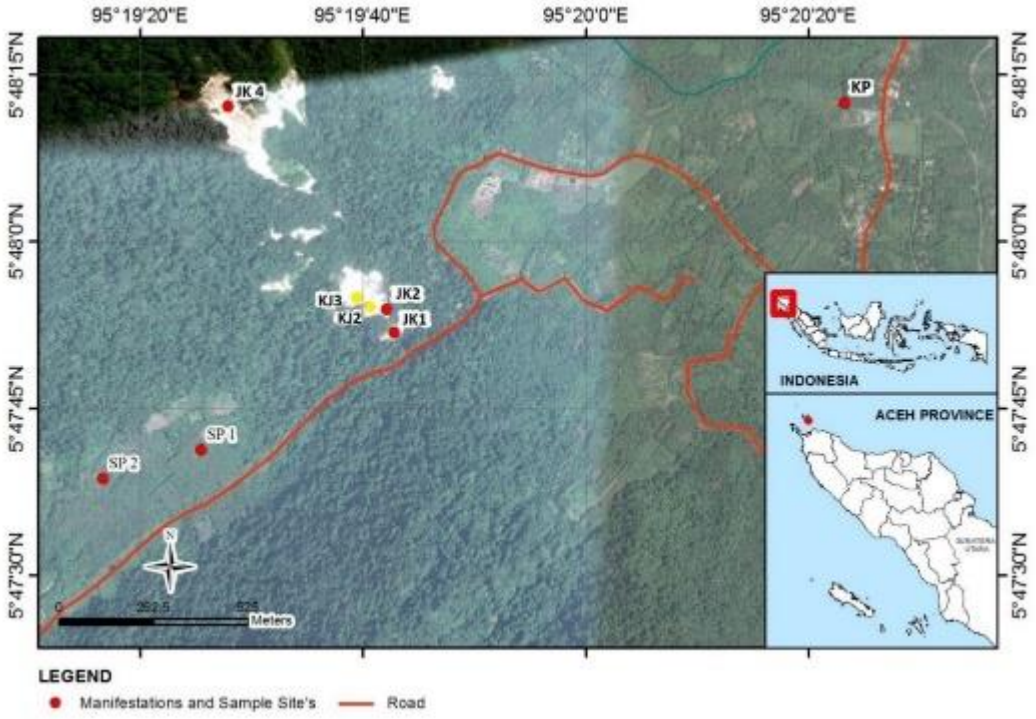

Fig.1 The satellite map of Jaboi manifestation, Sabang, Indonesia. (Yellow dots referred to fumarole. Red dots referred to manifestation)

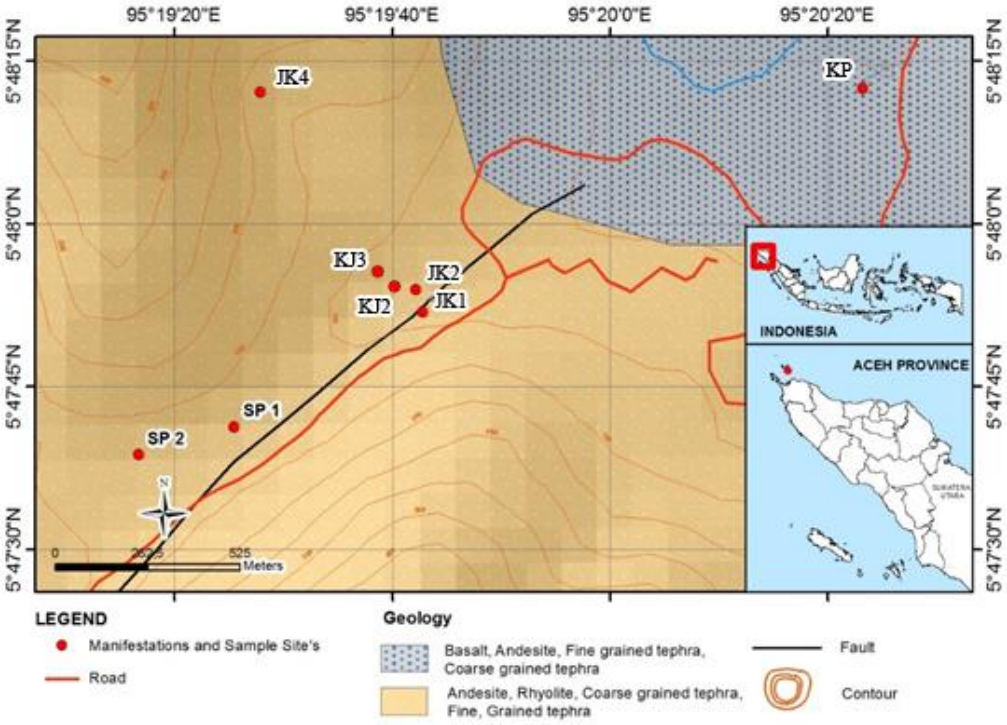

Fig.2 The geological map of Jaboi manifestation, Sabang, Indonesia.

The in-situ analysis was conducted at each sampling point. The analysis includes the measurement of surface water temperature with a portable thermometer (Fisher Scientific Traceable), acidity with pH-meter (Schott Instrument), conductivity with conductometer (Schott

Instrument) and Total Dissolved Solids (TDS) with TDS-meter (Hanna). The measurements were conducted with five repetitions to obtain the average value and the standard deviation.

Cation (K, Na, Mg, Ca, Li, and B) and anion (Cl and SO_4) were analyed by Ion Chromatography (Metrohm, IC Plus 883). Cation analysis was performed by using a column of Metrosep C4 250/4.0, eluent composition of 1 mmol/L HNO3 + 3.2 mmol/L dipocolinic acid dissolved in a double-distilled water, flow rate of 0.900 mL/min, and pressure of 9.63 MPa. Anion analysis were performed by using the column of Metrosep A Supp 5-150/4.0, eluent composition of 1 mmol/L $NaHCO_3$ + 3.2 mmol/L Na_2CO_3 dissolved in a double-distilled water and acetone (980 mL double-distilled water and 20 mL acetone), flow rate of 0.600 mL/min and pressure of 9.63 MPa. The SiO_2 analysis was carried out by a UV-Vis spectrophotometer (Thermo Scientific, Genesys 10S) with APHA standardized method [36]. The HCO_3^- analysis was conducted with alkalimetry titration using a methyl red indicator.

Isotope analysis (δD and $\delta^{18}O$) was conducted by Laser Absorption Spectrophotometer (LGR DLT-100 Liquid Water Stable Isotope Analyzer). The water samples were determined according to the calibration and control standards. The obtained value of the isotope ratio was converted to the international standard graph VSMOW [Vienna Standard Mean Ocean Water], with the analysis precision standard below 0.6 ‰ for δD and 0.1 ‰ for $\delta^{18}O$ [37].

3.2 Geothermal Gas Sampling

Gas samples were collected from the fumarole sources in the sampling point around the Jaboi crater (KJ2 and KJ3). The samples were collected into Giggenbach flasks with a standard gas sampling technique as explained by Giggenbach and Goguel [38]. Giggenbach bottles, filled with 100 mL NaOH 6 N, were kept under vacuum. A condensate vessel was connected, and the leaking check was conducted on the hose connecting the gas source with a Giggenbach bottle to prevent any contaminations from the outer air. The valve of the Giggenbach bottle was opened to let the gas flow into the bottle while being shaken to fasten the gas dissolution process in a NaOH solution. This process was ended when the vacuum was about to be run out in the Giggenbach bottle. The gas samples collected were carried to the laboratory for analysis. Gas sample analysis in a laboratory was conducted with two methods; gas chromatography method for unreactive gases (H_2, Ar, N_2, He, F, Cl, CH_4) using GC-TCD (HP-5890) with column porapak and titration method for reactive gases (CO_2, NH_3 and H_2S). H_2S analysis was carried out through sulphide ion titration by iodometry [39].

3.3 Geothermometer

3.3.1 Equations of Water Geothermometer

For the water sample, the depth temperature of the reservoir was estimated by using Na-K [40–45] and Na-K-Ca [46] geothermometers that can be seen in Table 1. The dominant chemical composition, water type, fluid equilibrium and the source of water were determined by Piper [39], Cl-SO_4-HCO_3 triangle, Na-K-Mg triangle [40] and Cl-Li-B diagrams, respectively.

Table 1 Water geothermometer equations.

Geothermometers	Equations (°C)	References
Na – K	T = [855.6 / (0.857 + log(Na/K))] – 273	[43]
Na – K	T = [833 / (0.780 + log(Na/K))] – 273	[42]
Na – K	T = [1319 / (1.699 + log(Na/K))] – 273	[45]
Na – K	T = [1217 / (1.483 + log(Na/K))] – 273	[41]
Na – K	T = [1178 / (1.470 + log(Na/K))] – 273	[44]
Na – K	T = [1390 / (1.750 + log(Na/K))] – 273	[40]
Na-K-Ca	$T = \frac{1647}{\log\frac{Na}{K} + \beta\left[\log\left(\frac{Ca^{1/2}}{Na}\right) + 2{,}06\right]} - 273$ for : β = 4/3, if T < 100 °C; β = 1/3, if T > 100 °C	[46]

3.3.2 Equations of Gas Geothermometer

The estimation of depth temperature of sampled gases was carried out by gas geothermometer equations that can be seen in Table 2. The depth temperature was also estimated by using CH_4/CO_2-H_2/Ar [47] and Fischer Tropsch-HSH (FT-HSH) diagrams [48]. The gas origin was estimated by the N_2-He-Ar triangle diagram [49]. The diagram was generated with the working sheet Gas_Analysis_v1_Powell-2010-StanfordGW.xls [50].

Table 2 Temperature equations (°C) for gas geothermometers.

Geothermometers	Equations (°C)	References
$CO_2/H_2S/CH_4/H_2$	$T = \frac{24775}{\left[2\log\left(\frac{CH_4}{CO_2}\right) - 6\log\left(\frac{H_2}{CO_2}\right) - 3\log\left(\frac{H_2S}{CO_2}\right) + 7\log P_{CO_2} + 36.05\right]} - 273.15$	[51]
CO_2	$T = -44.1 + 269.25\log m_{CO_2} - 76.88\left(\log m_{CO_2}\right)^2 + 9.52\left(\log m_{CO_2}\right)^3$	[52]
H_2S	$T = 246.7 + 44.81\ \log m_{H_2S}$	[52]
H_2S/H_2	$T = 304.1 + 39.48\ \log m_{H_2S/H_2}$	[52]
H_2/Ar	$T = 70\left[2.5 + \log\left(m_{H_2}/m_{Ar}\right)\right]$	[38]
CH_4/CO_2	$T = \frac{4625}{10.4 + \log\left(CH_4/CO_2\right)} - 273.15$	[49]
CO_2/H_2	$T = 341.7 + 28.57\ \log m_{CO_2/H_2}$	[49]

m = concentration (mmol/l)
P = pressure
T = temperature

4. RESULTS AND DISCUSSION

4.1 Characteristics of Manifestation Surface Water

The result of in-situ measurements such as temperature, pH, conductivity, TDS, and salinity as characteristic surface data of each geothermal hot spring manifestations in Jaboi manifestation can be seen in Table 4. The water on the production well (SP1) and Jaboi crater (JK1, JK2 and JK4) showed the high temperature at 84 °C, 70 °C, 79 °C and 90 °C, respectively, whereas the temperature of the water on injection well (SP2) and hot spring pond (KP) are warm at 39 °C and 57 °C, respectively.

3.4 Measurement Uncertainty

The uncertainty of measurement of each concentration analysis was stated by the standard deviation of the concentration (Sc) and other statistical function data. The calculation was done by using LINEST in Microsoft Excel software to obtain the standard deviation of the concentration (Sc), the mean of a set of M replicate analyses of unknowns (Y_c), the mean value of Y for the N calibration points (Y_{ave}), the sum of the squares of the deviations from the mean for individual values of x (S_{xx}), slope (m), the standard deviation of slope (Sm), intercept (b), replicated (M), count (N) and standard deviation of regression (Sr) [53]. The equations used in the calculation of the standard deviation of the concentration was shown in Table 3.

Table 3 The equation to calculate the standard deviation of the concentration.

Parameter	Equation	Reference
The standard deviation of the concentration	$Sc = \frac{S_r}{m}\sqrt{\frac{1}{M} + \frac{1}{N} + \frac{(Y_c - Y_{ave})^2}{m^2 S_{xx}}}$	[53]

The pH of water on the production well, injection well and hot spring pond are neutral, while the pH of water on the Jaboi crater is highly acidic up to 2. The high acidity of water around the crater was caused by the contact between water and fumarole [54] that induced the dissolution of gases into water.

The conductivity and TDS of all water samples were relatively low, except the water on hot spring pond that showed high one up to 1892 µS/cm and 1002 mg/l, respectively. The high conductivity and TDS on hot spring pond might be caused by human activity that utilizes the water for bathing.

Table 4 In-situ analysis of Jaboi manifestation.

Location	Code	Coordinate		Elevation (m)	T_{water} (°C)	pH	Conductivity (μS/cm)	TDS (mg/l)
		E	N					
Production Well	SP1	95°19'25"	5°47'42"	130	84 ± 0.01	7.42 ± 0.02	75.1 ± 0.13	37.5 ± 0.10
Injection well	SP2	95°19'22"	5°47'42"	129	40 ± 0.01	7.41 ± 0.01	35.6 ± 0.13	18.0 ± 0.11
Hot Spring Pond	KP	95°20'21"	5°48'12"	19	57 ± 0.01	6.36 ± 0.02	1892 ± 3	1002 ± 34
Jaboi Crater 1	JK1	95°19'40"	5°47'53"	85	70 ± 0.10	2.54 ± 0.01	18.61 ± 0.23	9.63 ± 0.02
Jaboi Crater 2	JK2	95°19'39"	5°47'56"	83	79 ± 0.02	2.29 ± 0.01	18.05 ± 0.10	9.04 ± 0.01
Jaboi Crater 4	JK4	95°19'26"	5°48'12"	176	96 ± 0.02	2.66 ± 0.01	4.89 ± 0.01	2.76 ± 0.04

4.2 Cation and Anion Contents of The Geothermal Water

Tables 5 and 6 exhibits the results of cation and anion concentration analysis. These data were then used to estimate the depth temperature with Na-K-Ca and Na-K geothermometer equations and determine the water's chemical equilibrium and water type.

Table 5 Cation concentration in the water of Jaboi manifestation.

Code	$[Na^+]$ ± Sc (mg/L)	$[K^+]$ ± Sc (mg/L)	$[Ca^{2+}]$ ± Sc (mg/L)	$[Mg^{2+}]$ ± Sc (mg/L)	$[Li^+]$ ± Sc (mg/L)	$[B^+]$ ± Sc (mg/L)	$[SiO_2]$ ± Sc (mg/L)
SP1	3081.52 ± 5.03	443.74 ± 2.06	960.51 ± 3.44	50.21 ± 0.77	8.15 ± 0.06	130.00 ± 0.01	15.64 ± 3.72
SP2	2781.37 ± 4.78	394.33 ± 1.94	2799.47 ± 5.84	278.64 ± 1.34	9.58 ± 0.07	136.00 ± 0.01	11.70 ± 3.38
KP	70.88 ± 0.90	12.77 ± 0.47	65.87 ± 1.00	45.20 ± 0.75	0.04 ± 0.02	0.85 ± 0.02	7.77 ± 2.99
JK1	274.32 ± 1.57	60.94 ± 0.82	708.48 ± 2.96	99.07 ± 0.92	1.31 ± 0.02	4.43 ± 0.01	115.5 ± 3.36
JK2	62.04 ± 0.86	9.32 ± 0.44	74.51 ± 1.05	17.94 ± 0.65	0.33 ± 0.01	0.04 ± 0.01	100.5 ± 3.22
JK4	22.93 ± 0.65	11.21 ± 0.45	178.16 ± 1.54	29.12 ± 0.69	0.29 ± 0.01	1.24 ± 0.02	23.9 ± 2.23

Table 6 Anion concentration in the water of Jaboi manifestation.

Code	[SO42-] (mg/L) ± Sc	[HCO3-] (mg/L) ± Sc	[Cl-] (mg/L) ± Sc
SP1	155.82 ± 0.70	88.50 ± 2.04	7045.38 ± 1.96
SP2	179.91 ± 0.75	87.46 ± 2.47	8867.49 ± 2.20
KP	339.48 ± 1.02	271.32 ± 0.89	36.64 ± 0.17
JK1	8036.04 ± 0.51	ttd	219.36 ± 0.36
JK2	4281.98 ± 3.58	ttd	3.11 ± 0.10
JK4	3209.47 ± 3.10	ttd	3.91 ± 0.10

4.3 Isotope Content of The Geothermal Water

The isotope values were given by the measurement of oxygen isotope ($\delta^{18}O$) and deuterium ($\delta^{2}H$) for the Jaboi manifestation which can be observed in Table 7.

Table 7 The value of isotope $\delta^{18}O$ and $\delta^{2}H$ in Jaboi manifestation.

Code	δD (‰)	$\delta^{18}O$ (‰)
SP1	-6.1 ± 2.1	8.34 ± 0.28
SP2	-0.7 ± 3.2	9.18 ± 0.42
KP	-20.0 ± 2.6	-3.09 ± 0.25
JK1	7.4 ± 3.5	9.23 ± 0.20
JK2	26.6 ± 1.6	13.20 ± 0.28
JK4	10.3 ± 0.6	6.46 ± 0.45

4.4 Content of the Geothermal Gas

The condensable gas and non-condensable gas analysis were calculated in the millimole (mmol/l) unit. The composition of fumarole in the Jaboi crater can be seen in table 8. It was found that the CO_2 content was dominant compared to other ones. The CO_2 content at KJ3 was higher than KJ2. This caused by the higher steam at KJ3 (1157.0 mmol/l) than KJ2 (834.8 mmol/l).

Table 8 Gases content on fumarole of Jaboi crater.

Source	Location	Code	Coordinate		Eleva-tion (m)	mmol/l										
			E	N		steam	CO_2	H_2S	NH_3	CH_4	N_2	Ar	He	H_2	Cl	F
Fuma -role	Jaboi crater	KJ2	95°19'39	05°47'55	83	834.8	163.9	25.4	0.32	1.25	2.95	0.017	0.006	5.66	29.2	0.01
		KJ3	95°19'36	05°47'57	85	1157.0	217.2	4.9	2.29	1.49	3.96	0.014	0.005	6.74	38.3	0.008

5. DISCUSSION

5.1 Geochemical Process of the Geothermal Water

5.1.1 Dominant Chemical Composition and The Type of Geothermal Water

The determination of dominant chemical compositions in the water is stated by the Piper diagram (fig 3). It can be seen that the waters in Jaboi Crater (JK1, JK2, and JK4), hot spring pond (KP) and production-injection well (SP1 and SP2) have dominant of calcium-sulfate ($Ca\text{-}SO_4$), magnesium-bicarbonate-sulfate ($Mg\text{-}HCO_3\text{-}SO_4$) and sodium-calcium-chloride (Na-Ca-Cl), respectively.

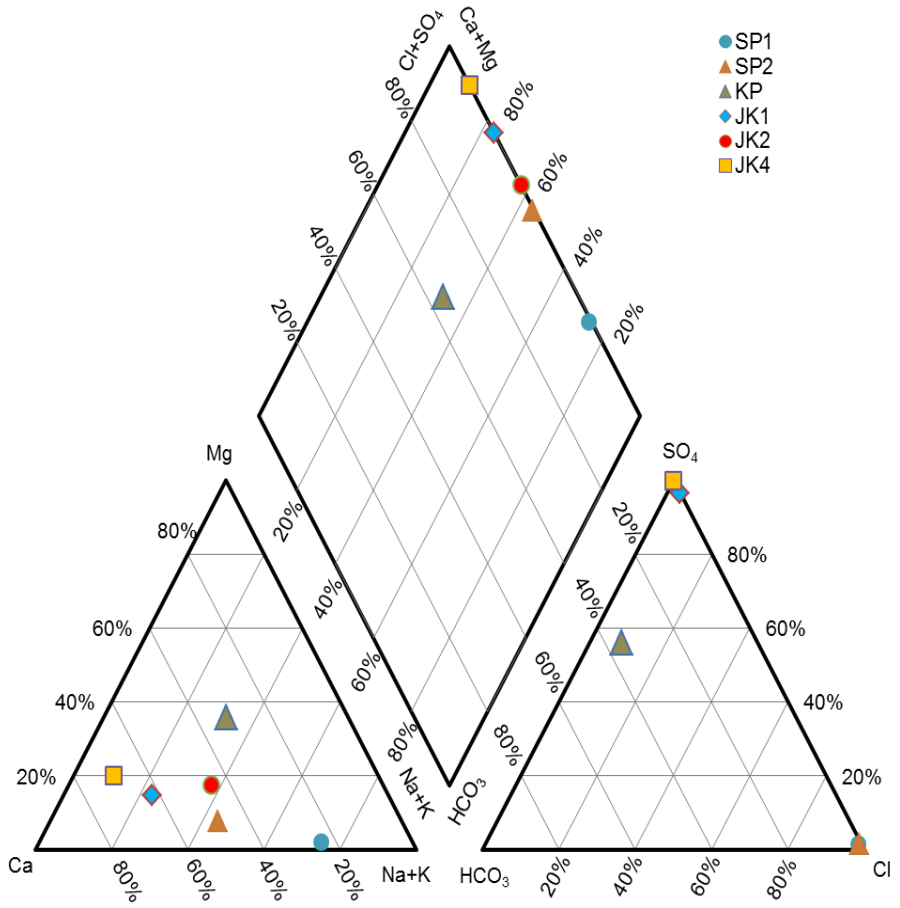

Fig.3 Piper diagram for chemical dominant compositions.

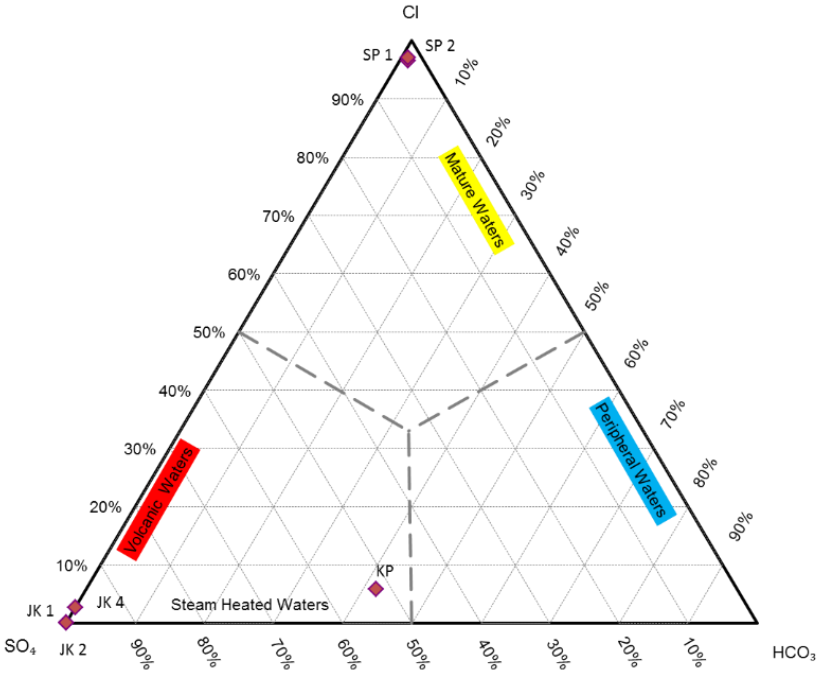

Fig.4 Cl-HCO_3-SO_4 triangle diagram for the water type.

The water type was conducted based on the dominant anion content in the sample, explained by the Cl-HCO_3-SO_4 triangle diagram [40]. It can be seen in fig 4 that the water in production-injection well (SP1 and SP2) is mature water of Chloride type. The manifestations in the Jaboi crater are steam-heated water of sulfate type. The high SO_4 content is caused by the contribution of volcanic fluids, being very acidic and sulfate-rich, whereas the HCO_3-rich waters are the typical peripheral waters of volcanic systems due to CO_2 dissolution [55], [56]. The mixed bicarbonate-sulfate water type was found in the hot spring pond. It might be ascribed to the dissolution of H_2S into groundwater when it emerges to the surface at low temperature [57].

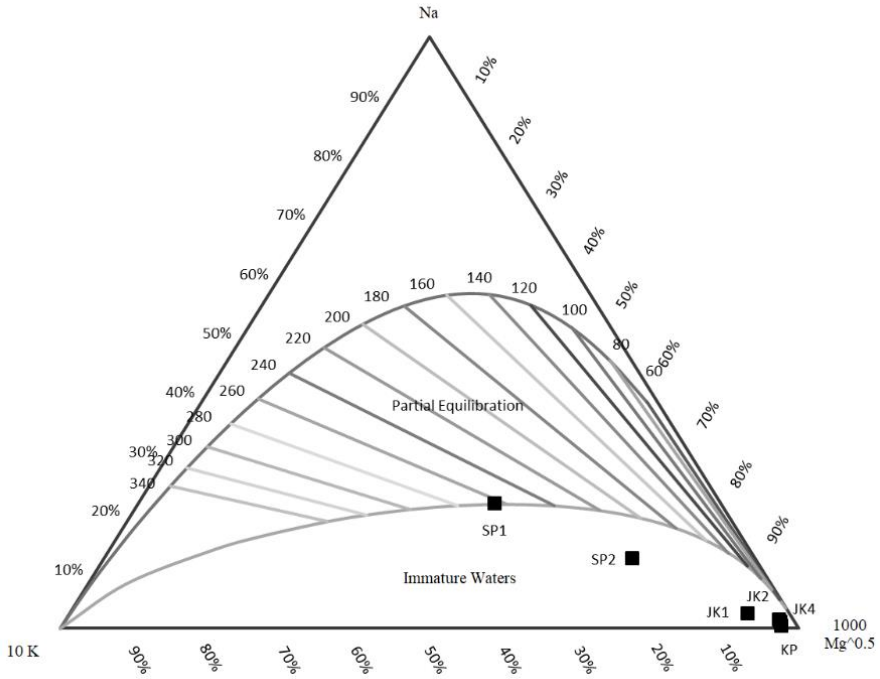

Fig.5 Na-K-Mg triangle diagram of Jaboi manifestation

5.1.2 Fluid Equilibrium of the Geothermal Water

The fluid equilibrium was determined based on the ratio of Na/K and K/Mg from the dissolution of albite, K-feldspar, illite, chlorite, and silica (chalcedony or quartz) in geothermal water, explained by Na-K-Mg triangle diagram [40].

It can be seen in Fig 5 that the water in the production well (SP1) is located at the partial equilibration lines, which is the characteristic of mature water. This is ascribed to the mineral dissolution, especially Na and K, has reached an equilibrium in the reservoir. So that, when the water emerged to the surface, mixing of other minerals is no longer affecting the equilibrium [58].The fluid equilibrium at the injection well (SP2), Jaboi crater (JK1, JK2 and JK4) and hot spring pond (KP) are located in the immature waters. This indicated that the geothermal waters are not in equilibrium. This condition indicates that there is an influence of volcanic waters (hot, acidic, sulphate-rich). The samples probably depict a mixing between two endmembers: a mature hydrothermal water and a volcanic water [56], [59]. Hence, the use of triangle Na-K-Mg to estimate the depth temperature is not suitable for this system.

5.1.3 Source of the Geothermal Water

The Cl-Li-B triangle diagram is used to indicate the source of water composition based on the concentration ratio of Cl, Li, B [49].

It can be seen in fig 6 that the geothermal waters in the production-injection well (SP1 and SP2) and hot spring pond (KP) are close to the upper B-Cl side. This implied waters from a mature hydrothermal system which is in agreement with the plot in Fig.5. The waters also showed an equal ratio of Cl/B that was caused by the high interception on Cl concentration, probably formed from the marine sedimentary rocks water.

From Fig. 6, it can be seen that the water in JK2 is Li-rich water and the waters in JK1 and JK4 have an equal ratio of Li/B and Cl/Li/B, respectively. These gave again the evidence of the contribution of magmatic fluids causing rock dissolution and Li extraction. In contrast with JK1, JK2 and JK4, the waters in SP1, SP2 and KP are related to a more mature hydrothermal contribution. Probably, some degree of mixing occurs between these two endmembers of mature hydrothermal water and a volcanic water.

5.2 Estimation of Reservoir Temperature

5.2.1 Water Geothermometer

Geothermometer Na-K **[**40–45] is used to estimate the reservoir temperature based on the ratio of Na and K contents in the geothermal water. This geothermometer is well applied for temperature estimation in the range of 180-350 °C or less than 120 °C [60].

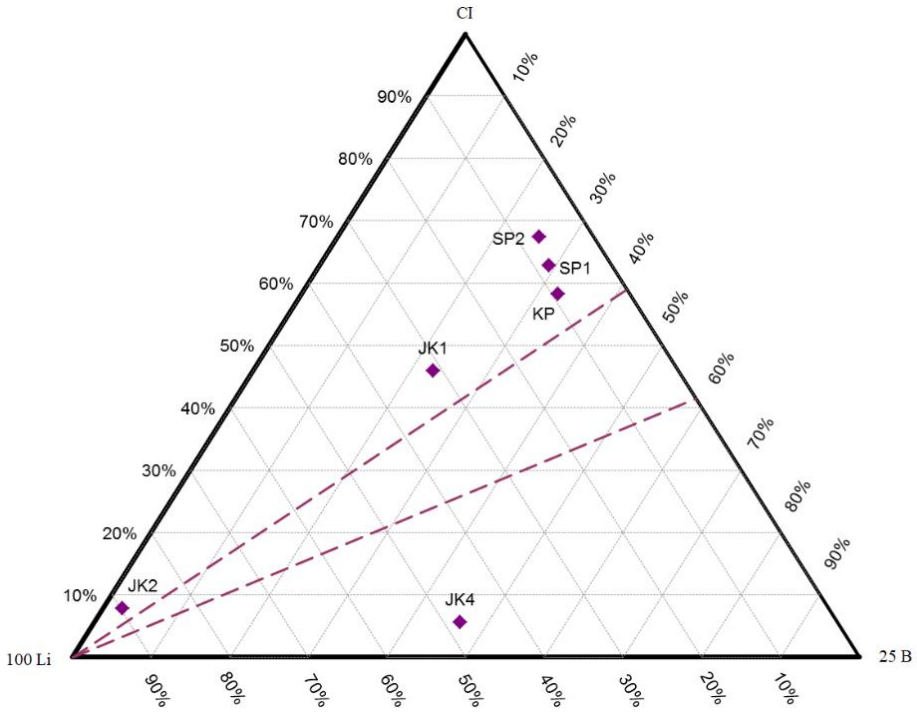

Fig.6 Cl-Li-B triangle diagram of Jaboi manifestation

Table 9 Reservoir temperature estimation of each geothermal water in Jaboi manifestation.

Code	Na-K-Ca (Fournier & Truesdell (1973) (°C)	Na/K Fournier (1979) (°C)	Na/K Truesdell (1976) (°C)	Na/K Giggenbach (1988) (°C)	Na/K Tonani (1980) (°C)	Na/K Nieva & Nieva (1987) (°C)	Na/K Arnorsson (1983) (°C)
SP1	222	251	231	264	272	237	236
SP2	201	248	227	261	268	234	232
KP	77	276	265	287	311	262	268
JK1	92	299	297	308	348	284	297
JK2	60	239	216	253	255	225	222
JK4	45	416	478	411	558	399	458

The reservoir temperatures can be observed in Table 9 with several geothermometers Na-K. Except for the sampling point of KJ4, the reservoir temperatures in other sampling points were in the range of 180-350 °C, thus the estimation is suitable to perform by only one geothermometer. Based on the geothermometer of Na-K Giggenbach [40], the reservoir temperatures of manifestation in sampling points of SP1, SP2, JK1, JK2 and KP are 264 °C. 261 °C, 308 °C, 253 °C, and 287 °C, respectively. Meanwhile, the estimation of the reservoir temperature of more than 350 °C in the sampling point of JK4 is more suitable by using Na/K Fournier [41]. The reservoir at that sampling point is 416 °C.

5.2.2 Gas Geothermometer

There are several types of manifestation around Jaboi crater, which are fumarole, solfatara, hydrothermal alteration, hot spring (acid) and mud pool. However, the only fumarole has the dominant steam that is suitable to investigate the reservoir temperature. It can be seen in table 10 that the reservoir temperature in the Jaboi crater calculated by several gas geothermometers [31,42,44,45] is in the range of 222 °C - 351 °C for KJ2 and 196 °C - 362 °C for KJ3.

Table 10 Reservoir temperature estimations of gas geothermal in Jaboi manifestation.

Location	Code	Gas Geothermometer (T = °C)						
		$CO_2/H_2S/CH_4/H_2$	CO_2	H_2S	H_2S/H_2	H_2/Ar	CH_4/CO_2	CO_2/H_2
Jaboi	KJ2	222	278	309	278	351	285	299
Crater	KJ3	196	286	277	309	362	288	298

5.2.3 CH_4/CO_2-H_2/Ar Diagram and Fischer-Tropsch-Pyrite-Magnetite (FT-HSH) Diagram

CH_4/CO_2-H_2/Ar diagram [47] estimated the reservoir temperature based on the ratio of $CO_2/CH_4/H_2$/Ar concentration ratio, while the FT-HSH diagram [48] estimated it based on a gas release (degassing) by geothermal fluid during emerging to the surface [50]. Based on the CH_4/CO_2-H_2/Ar diagram (Fig 7A), the fumaroles of both Jaboi crater sampling points are located on the temperature line between 275 – 300 °C. Based on the FT-HSH diagram (Fig 7B), the fumaroles of KJ2 and KJ3 are located at 325 – 350 °C and 250 – 275 °C, respectively. Both Fig 7A and 7B show that KJ fumaroles fall in the two-phase field of coexisting liquid-vapor. Both the figs thus suggest that the fumaroles are mixed liquid-vapor systems, flashed by decompression. Based on both diagrams, it can be concluded that the reservoir temperature in Jaboi manifestation is around 250-350 °C.

5.2.4 N_2-He-Ar Triangle Diagram

Triangle diagram N_2-He-Ar is a mixing model diagram to portray the relative contribution of gas sources, whether the gas is originated from magmatic, meteoric or earth crust. Content proportions of N_2, He, and Ar have been combined by Giggenbach [48] for the identification of dominant gas sources at the fumarole manifestation in the geothermal system [60]. Based on Fig 8, the Jaboi crater's fumarole is suggested to be originated from a mixed gas, where contributions from magmatic gases, crustal and air components are evident.

5.3 Isotope Plot

Isotope values are connected to the international standard lines V-SMOW to explain the origin of the geothermal water, whether the water is meteoric, magmatic or a mixture of both [60,61]. Based on the stable isotope plot (Fig 9), the water of hot spring pond (KP) is originated from meteoric water.

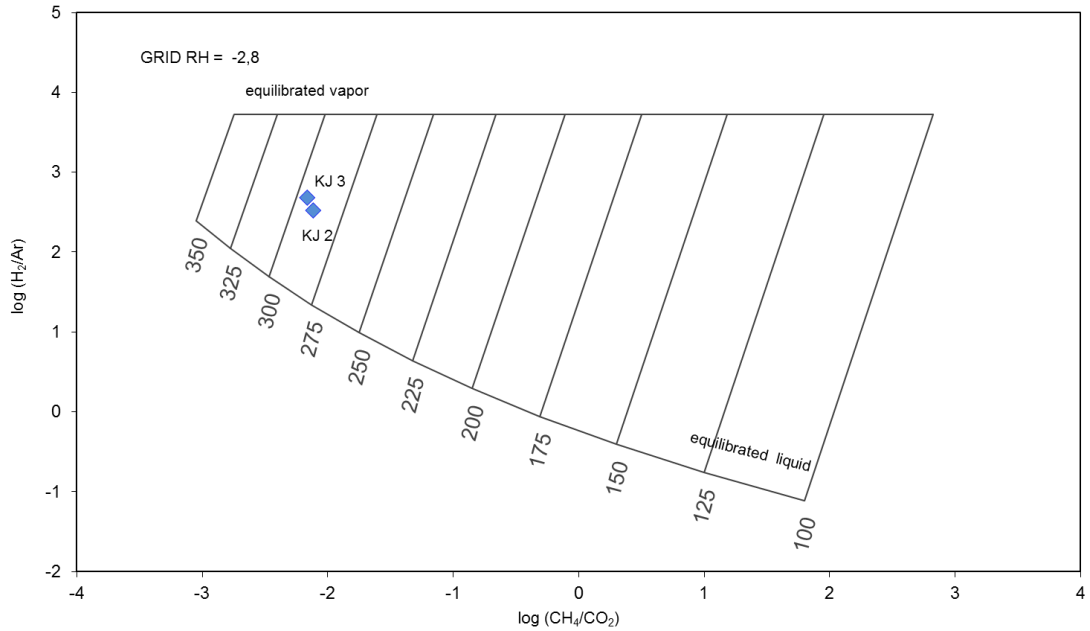

A

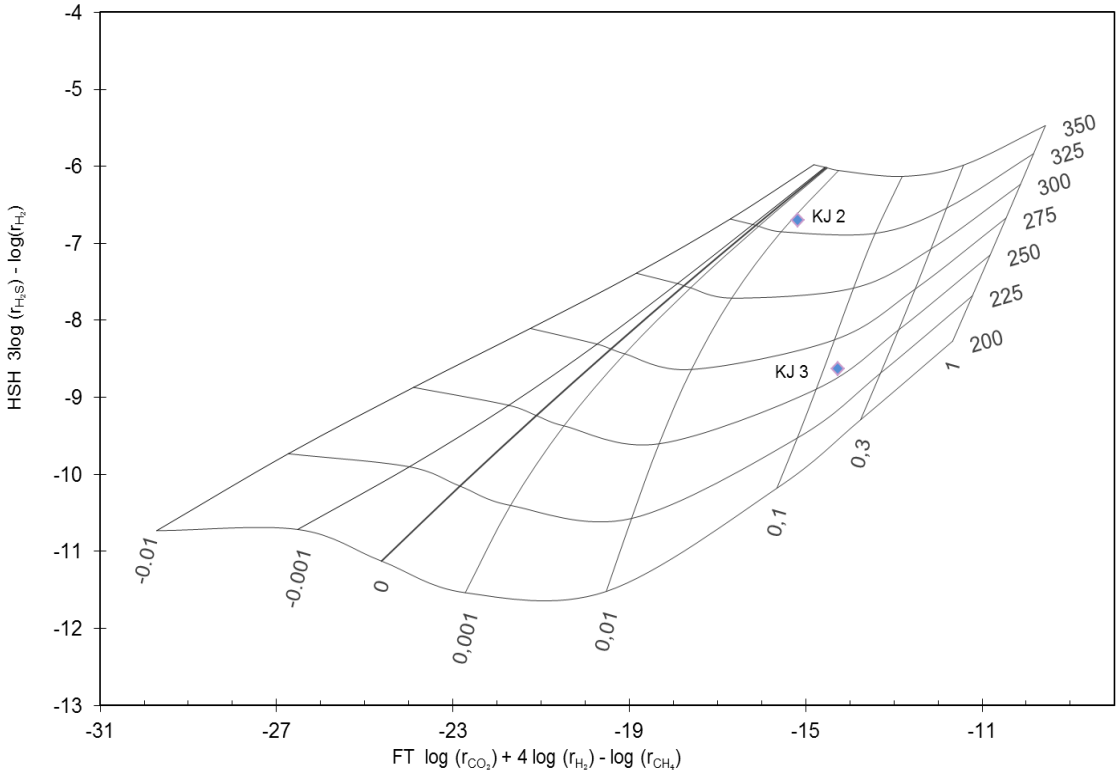

B

Fig.7 (A) CH_4/CO_2-H_2/Ar diagram; (B) FT-HSH diagram (r: the gas/steam ratio).

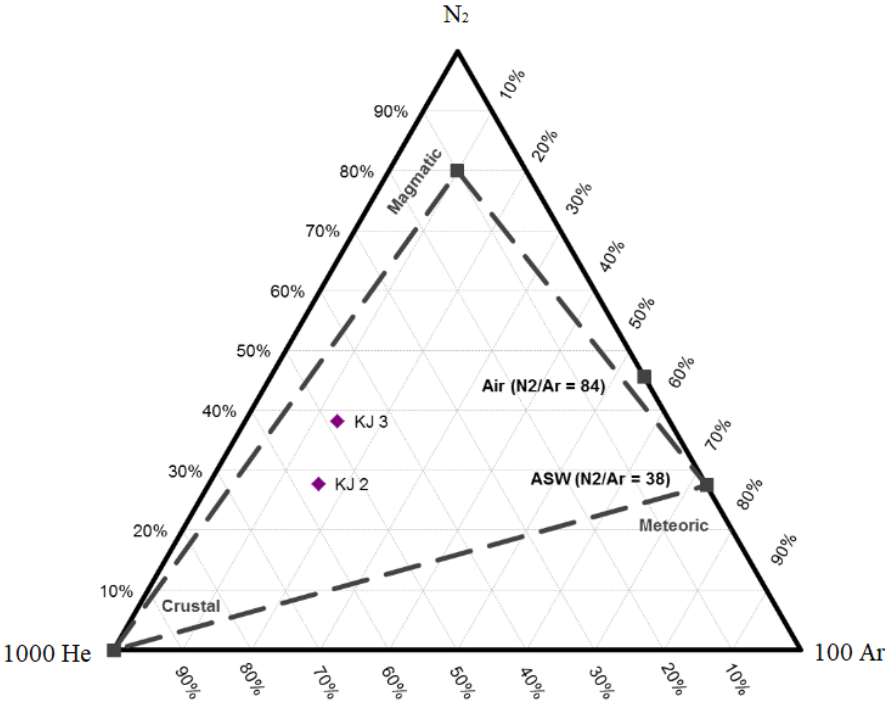

Fig.8 N_2-He-Ar triangle diagram

This is indicated by the relatively negative isotope value, which is close to LMWL (local meteoric water line). The water of the production-injection well (SP1 and SP2) showed a mixture of both magmatic and meteoric water. This indicated by the positive value of isotope $\delta^{18}O$, while the isotope δD is negative. The water in Jaboi crater (JK1, JK2, and JK4) are originated from magmatic water. This is due to the fact that the isotope value found to be positive. The change of isotope value to the positive direction is, caused by the shifting reaction of the heavier isotope δD that allowed the contribution of magmatic water [62]. This occurrence is also found in Ijen Crater (Jawa Timur) with an assumption that the meteoric fluids are affected by the change of isotope due to the high temperature and mixed with the volcanic fluids [59].

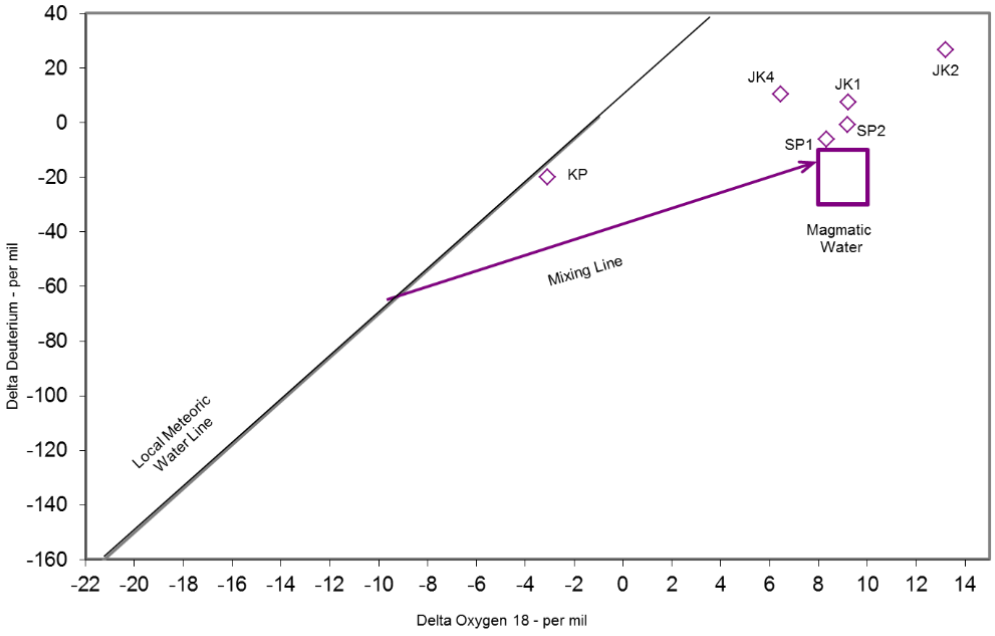

Fig.9 $\delta^{18}O$ and $\delta^{2}H$ stable isotope plot [47]

6. CONCLUSIONS

Having some volcano systems in Aceh provide a geothermal energy potential. This renewable energy can resolve the global fossil fuel problem. However, the geothermal potential mostly hasn't exploited yet. To achieve this purpose, several exploration procedure must be done including geochemical study. The study is required to obtain the temperature reservoir and physical-chemical characteristics of geothermal system.

The geochemical studies of the Jaboi manifestations, Sabang concern three sub-areas, that are production-injection well of PT. Sabang Geothermal Energy, Jaboi crater, and hot spring pond. Based on Piper and Cl-HCO_3-SO_4 diagram, the dominant chemical composition and water type are (1) chloride for production-injection well, (2) sulfate for Jaboi crater, and (3) mixture of bicarbonate-sulfate for hot spring pond (KP).

Based on the Na-K-Mg diagram, the fluid equilibrium of the water in the production well (SP1) is mature water. Meanwhile, the waters in the injection well (SP2), Jaboi crater (JK1, JK2 and JK3) and hot spring pond (KP) are immature water.

Based on the Cl-Li-B diagram, the source of water composition at the production-injector well and hot spring pond is the marine sedimentary rocks water, a mixture between the meteoric and seawater. The water of Jaboi crater in JK4 and JK1 showed the presence of magmatic gas absorption, while in JK2 there was Cl absorption by Li from the hot rocks into reservoir water. Based on stable isotope plot, the water origins of jaboi manifestation are (1) mixture of both magmatic and meteoric for production-injection well, (2) magmatic for Jaboi crater, and (3) meteoric for hot spring pond. Based on the N_2-He-Ar triangle diagram, the gas origin of fumarole in the Jaboi crater is from the earth's crust.

Based on the geothermometer of Na-K Giggenbach [40], the reservoir temperatures of Jaboi manifestation in production well, injection well, Jaboi crater JK1, Jabor crater JK2 and hot spring pond are 264 °C, 261 °C and, 308 °C, 253 °C, and 287 °C, respectively. Based on the geothermometer Na-K Fournier [41], it indicated that water in Jaboi crater JK4 has reservoir temperature at 416 °C.

Based on gas geothermometer, reservoir temperature in Jaboi manifestation are in the range of 222 °C - 351 °C for KJ2 and 196 °C - 362 °C for KJ3. Based on CH_4/CO_2-H_2/Ar and FT-HSH diagram, the reservoir temperature in Jaboi manifestation is around 250-350 °C.

Based on the reservoir temperature, estimated well by the gas geothermometers and water geothermometer, Jaboi manifestation in Sabang, Aceh Province, Indonesia is classified as a high temperature (High Enthalpy) geothermal system, indicated by the obtained average reservoir temperature of >225 °C. This condition suggests that the geothermal area is suitable for power plant development.

7. ACKNOWLEDGMENTS

We would like to thank Ir. Martoyo Head of Geothermal Engineering PT. Sabang Geothermal Energy. We would also like to thank Andi lala, Mahmudi, Rivansyah Suhendra, Aga Maulana, Ghazi Mauer Idroes and Prof. Teuku Meurah Indra Mahlia for their technical supports.

8. FUNDING

This research was funded by Kementerian Pendidikan dan Kebudayaan through "Penelitian Dasar" scheme, grant number: 78/UN11.2.1/PT.01.03/AMD/DPRM/2020 and by Universitas Syiah Kuala, Kementrian Riset, Teknologi dan Pendidikan Tinggi through "Penelitian Lektor Kepala" scheme, grant number: 521/UN11/SPK/PNBP/2019.

9. REFERENCES

[1] Ong H. C., Masjuki H. H., Mahlia T. M. I., Silitonga A. S., Chong W. T., and Yusaf T., Engine performance and emissions using Jatropha curcas, Ceiba pentandra and Calophyllum inophyllum biodiesel in a CI diesel engine. Energy. Vol. 69. 2014, pp. 427–445.

[2] Silitonga H. H.; Mahlia, T. M. I.; Ong, H. C.; Chong, W. T A. S. . M., Experimental study on performance and exhaust emissions of a diesel engine fuelled with Ceiba pentandra biodiesel blends. Energy Conversion and Management. Vol. 76. 2013, pp. 828–836.

[3] Ismail M. S., Moghavvemi M., and Mahlia T. M. I., Techno-economic analysis of an optimized photovoltaic and diesel generator hybrid power system for remote houses in a tropical climate. Energy Conversion and Management. Vol. 69. 2013, pp. 163–173. doi: 10.1016/j.enconman.2013.02.005.

[4] Ismail M.; Mahlia, T. M. I. M. S. . M., Characterization of PV panel and global optimization of its model parameters using genetic algorithm. Energy Conversion and Management. Vol. 73. 2013, pp. 10–25.

[5] Amin M., Putra N., Kosasih E. A., Prawiro E., Luanto R. A., and Mahlia T. M. I., Thermal properties of beeswax/graphene phase change material as energy storage for building applications. Applied Thermal Engineering. Vol. 112. 2017, pp. 273–280. doi: 10.1016/j.applthermaleng.2016.10.085.

[6] Latibari M.; Mehrali, M.; Mahlia, T. M. I.; Metselaar, H. S. C. S. T. . M., Synthesis, characterization and thermal properties of nanoencapsulated phase change materials via sol–gel method. Energy. Vol. 61. 2013, pp. 664–672.

[7] Mehrali S. T.; Mehrali, M.; Mahlia, T. M. I.; Metselaar, H. S. C. M. . L., Preparation and properties of highly conductive palmitic acid/graphene oxide composites as thermal energy storage materials. Energy. Vol. 58. 2013, pp. 628–634.

[8] Silitonga A. S., Mahlia T. M. I., Ong H. C., Riayatsyah T. M. I., Kusumo F., Ibrahim H., Dharma S., and Gumilang D., A comparative study of biodiesel production methods for Reutealis trisperma biodiesel. Energy Sources, Part A: Recovery, Utilization, and Environmental Effects. Vol. 39, Issue 20. 2017, pp. 2006–2014.

[9] Silitonga A. S., Masjuki H. H., Ong H. C., Sebayang A. H., Dharma S., Kusumo F., Siswantoro J., Milano J., Daud K., Mahlia T. M. I., Chen W.-H., and Sugiyanto B., Evaluation of the engine performance and exhaust emissions of biodiesel-bioethanol-diesel blends using kernel-based extreme learning machine. Energy. Vol. 159. 2018, pp. 1075–1087. doi: 10.1016/j.energy.2018.06.202.

[10] Silitonga A. S., Mahlia T. M. I., Kusumo F., Dharma S., Sebayang A. H., Sembiring R. W., and Shamsuddin A. H., Intensification of Reutealis trisperma biodiesel production using infrared radiation: Simulation, optimisation and validation. Renewable Energy. Vol. 133. 2019, pp. 520–527.

[11] Nasruddin, Idrus Alhamid M., Daud Y., Surachman A., Sugiyono A., Aditya H. B., and Mahlia T. M. I., Potential of geothermal energy for electricity generation in Indonesia: A review. Renewable and Sustainable Energy Reviews. Vol. 53. 2016, pp. 733–740. doi: 10.1016/j.rser.2015.09.032.

[12] Bertani R., Geothermics Geothermal power generation in the world 2010 – 2014 update report. Geothermics. Vol. 60. 2016, pp. 31–43. doi: 10.1016/j.geothermics.2015.11.003.

[13] Haryanto I., Ilmi N. N., Hutabarat J., Adhiperdana B. G., Fauzielly L., Sendjaja Y. A., and Sunardi E., Tectonic and geological structures of gunung kromong, west java, Indonesia. International Journal of GEOMATE. Vol. 19, Issue 74. 2020, pp. 185–193. doi: 10.21660/2020.74.05449.

[14] Ochieng L., Overview of geothermal surface exploration methods. 001374011. 2014, p.

[15] Supriyadi, Khumaedi, and Putro A. S. P., Geophysical and hydrochemical approach for seawater intrusion in north semarang, Central Java, Indonesia. International Journal of GEOMATE. Vol. 12, Issue 31. 2017, pp. 134–140. doi: 10.21660/2017.31.50405.

[16] Kristinsdóttir L. H., Flóvenz Ó. G., Árnason K., Bruhn D., Milsch H., Spangenberg E., and Kulenkampff J., Electrical conductivity and P-wave velocity in rock samples from high-temperature Icelandic geothermal fields. Geothermics. Vol. 39, Issue 1. 2010, pp. 94–105.

[17] Marwan, Idroes R., Yanis M., Idroes G. M., and Syahriza, A Low-Cost Uav Based Application for Identify and Mapping a Geothermal Feature in Ie Jue Manifestation, Seulawah Volcano, Indonesia. International Journal of GEOMATE. Vol. 20, Issue 80. 2021, p. doi: 10.21660/2021.80.j2044.

[18] Marwan M., Syukri M., Idroes R., and Ismail N., Deep and Shallow Structures of Geothermal Seulawah Agam Based on Electromagnetic and Magnetic Data. International Journal of GEOMATE. Vol. 16, Issue 53. 2019, pp. 141–147.

[19] Marwan M., Yanis M., Idroes R., and Ismail N., 2D Inversion and Static Shift of MT and TEM Data For Imaging the Geothermal Resources of Seulawah Agam Volcano, Indonesia. International Journal of GEOMATE. Vol. 17, Issue 62. 2019, pp. 173–180. doi: 10.21660/2019.62.11724.

[20] Idroes R., Yusuf M., Alatas M., Subhan, Lala A., Saiful, Suhendra R., Idroes G. M., and Marwan, Geochemistry of hot springs in the Ie Seu'um hydrothermal areas at Aceh Besar district, Indonesia. IOP Conference Series: Materials Science and Engineering. Vol. 334. 2018, p. 012002. doi: 10.1088/1757-899X/334/1/012002.

[21] Idroes R., Yusuf M., Alatas M., Subhan, Lala A., Muslem, Suhendra R., Idroes G. M., Suhendrayatna, Marwan, and Riza M., Geochemistry of warm springs in the Ie Brôuk hydrothermal areas at Aceh Besar district. IOP Conference Series: Materials Science and Engineering. Vol. 523. 2019, p. 012010. doi: 10.1088/1757-899X/523/1/012010.

[22] Idroes R., Yusuf M., Alatas M., Subhan, Lala A., Muhammad, Suhendra R., Idroes G. M., and Marwan, Geochemistry of Sulphate spring in the Ie Jue geothermal areas at Aceh Besar district, Indonesia. IOP Conference Series: Materials Science and Engineering. Vol. 523. 2019, p. 012012. doi: 10.1088/1757-899X/523/1/012012.

[23] Idroes R., Yusuf M., Saiful S., Alatas M., Subhan S., Lala A., Muslem M., Suhendra R., Idroes G. M., Marwan M., and Mahlia T. M. I., Geochemistry Exploration and Geothermometry Application in the North Zone

of Seulawah Agam, Aceh Besar District, Indonesia. Energies. Vol. 12, Issue 23. 2019, p. 4442. doi: 10.3390/en12234442.

[24] Isa M., Mat Jafri M. Z., and Lim H. S., Comparison of field temperature versus satellite temperature thermal band in geothermal area, in AIP Conference Proceedings, 2013, Vol. 1528, Issue 1, 2013, pp. 163–168.

[25] Darma S., and Gunawan R., Country update: geothermal energy use and development in Indonesia, in Proceedings World Geothermal Congress, Melbourne, Australia, 2015, 2015, pp. 19–25.

[26] Guo Q., Pang Z., Wang Y., and Tian J., Fluid geochemistry and geothermometry applications of the Kangding high-temperature geothermal system in eastern Himalayas. Applied Geochemistry. Vol. 81. 2017, pp. 63–75. doi: 10.1016/j.apgeochem.2017.03.007.

[27] Suhartono E., Thalib I., Aflanie I., Noor Z., and Idroes R., Study of Interaction between Cadmium and Bovine Serum Albumin with UV-Vis Spectrocopy Approach. IOP Conference Series: Materials Science and Engineering. Vol. 350, Issue 1. 2018, p. 12008. doi: 10.1088/1757-899X/350/1/012008.

[28] Lahna K., Idroes R., Idris N., Abdulmadjid S. N., Kurniawan K. H., Tjia M. O., Pardede M., and Kagawa K., Formation and emission characteristics of CN molecules in laser induced low pressure He plasma and its applications to N analysis in coal and fossilization study. Applied Optics. Vol. 55, Issue 7. 2016, p. 1731. doi: 10.1364/AO.55.001731.

[29] Marpaung A. M., Ramli M., Idroes R., Suyanto H., Lahna K., Abdulmadjid S. N., Idris N., Pardede M., Hedwig R., Lie Z. S., Kurniawan D. P., Kurniawan K. H., Lie T. J., Tjia M. O., and Kagawa K., A comparative study of emission efficiencies in low-pressure argon plasmas induced by picosecond and nanosecond Nd:YAG lasers. Japanese Journal of Applied Physics. Vol. 55, Issue 11. 2016, p. 116101. doi: 10.7567/JJAP.55.116101.

[30] Pardede M., Jobiliong E., Lahna K., Idroes R., Suyanto H., Marpaung A. M., Abdulmadjid S. N., Idris N., Ramli M., and Hedwig R., The underlying physical process for the unusual spectral quality of double pulse laser spectroscopy in He gas. Analytical chemistry. 2019, p.

[31] Tassi F., Aguilera F., Darrah T., Vaselli O., Capaccioni B., Poreda R. J., and Delgado Huertas A., Fluid geochemistry of hydrothermal systems in the Arica-Parinacota, Tarapacá and Antofagasta regions (northern Chile). Journal of Volcanology and Geothermal Research. Vol. 192, Issue 1–2. 2010, pp. 1–15. doi: 10.1016/j.jvolgeores.2010.02.006.

[32] Avşar Ö., Güleç N., and Parlaktuna M., Hydrogeochemical characterization and conceptual modeling of the Edremit geothermal field (NW Turkey). Journal of Volcanology and Geothermal Research. Vol. 262. 2013, pp. 68–79. doi: 10.1016/j.jvolgeores.2013.05.015.

[33] Wassenaar L. I., Ahmad M., Aggarwal P., Van Duren M., Pöltenstein L., Araguas L., and Kurttas T., Worldwide proficiency test for routine analysis of δ2H and δ18O in water by isotope-ratio mass spectrometry and laser absorption spectroscopy. Rapid Communications in Mass Spectrometry. Vol. 26, Issue 15. 2012, pp. 1641–1648.

[34] Soetoyo S., and Widodo S., Pengaruh Sesar Normal Ceunohot terhadap Landaian Temperatur Sumur Jbo-1 dan Jbo-2 di Lapangan Panas Bumi Jaboi, Sabang, Nanggroe Aceh Darussalam. Buletin Sumber Daya Geologi. Vol. 5, Issue 3. 2010, pp. 182–192.

[35] Abubakar M., Sugianto D., and Zainal M., Application of Resistivity Methods for Agriculture in Jaboi-Sabang Geothermal Area. Journal of Aceh Physics Society. Vol. 7, Issue 2. 2018, pp. 102–105.

[36] APHA., Standard Methods for the Examination of Water and Wastewater. 21st Edition. Washington DC: American Public Health Association/American Water Works Association/Water Environment Federation, 2005.

[37] Craig H., The isotopic geochemistry of water and carbon in geothermal areas, Nuclear geology on geothermal areas. Spoleto 1963. 1963, pp. 17–53.

[38] Giggenbach W. F., Collection and analysis of geothermal and volcanic water and gas discharges. NZ DSIR Chemistry Report. Vol. 2401. 1989, pp. 1–82.

[39] Pawlak Z., Modification of iodometric determination of total and reactive sulfide in environmental samples. Talanta. Vol. 48, Issue 2. 1999, pp. 347–353. doi: 10.1016/S0039-9140(98)00253-7.

[40] Giggenbach W. F., Geothermal solute equilibria. Derivation of Na-K-Mg-Ca geoindicators. Geochimica et Cosmochimica Acta. Vol. 52, Issue 12. 1988, pp. 2749–2765. doi: 10.1016/0016-7037(88)90143-3.

[41] Fournier R. O., A revised equation for the Na/K geothermometer. Transactions of the Geothermal Resources Council. Vol. 3. 1979, pp. 221–224.

[42] Tonani F. B., Some Remarks on the Application of Geochemical Techniques in geothermal exploration, in Advances in European Geothermal Research, Dordrecht: Springer Netherlands, 1980, 1980, pp. 428–443.

[43] Truesdell A. H., Geochemical Techniques in

Exploration: Summary of Section III, in Proceedings of the Second UN Symposium on the Development and Use of Geothermal Resources, *1975*, 1976, 1976, pp. Iiii–Ixxix.

[44] Nieva D., and Nieva R., Developments in geothermal energy in Mexico—part twelve. A cationic geothermometer for prospecting of geothermal resources. Heat Recovery Systems and CHP. Vol. 7, Issue 3. 1987, pp. 243–258. doi: 10.1016/0890-4332(87)90138-4.

[45] Arnórsson S., Chemical equilibria in icelandic geothermal systems—Implications for chemical geothermometry investigations. Geothermics. Vol. 12, Issue 2–3. 1983, pp. 119–128. doi: 10.1016/0375-6505(83)90022-6.

[46] Fournier R. O., and Truesdell, Empirical Na-K-Ca geothermometer for natural waters", Geochim. Cosmochim. Ac. Vol. 37. 1973, pp. 1255–1275.

[47] Giggenbach W. F., and Glover R. B., Tectonic regime and major processes governing the chemistry of water and gas discharges from the Rotorua geothermal field, New Zealand. Geothermics. Vol. 21, Issue 1–2. 1992, pp. 121–140.

[48] Giggenbach W. F., Geothermal gas equilibria. Geochimica et cosmochimica acta. Vol. 44, Issue 12. 1980, pp. 2021–2032.

[49] Giggenbach W. F., Isotopic composition of geothermal water and steam discharges. In: D'Amore, F. (Ed.). Application of Geochemistry in Geothermal Reservoir Development. 1991, pp. 253–273.

[50] Powell T., and William C., Spreadsheets for Geothermal Water and Gas Geochemistry In: Proceedings, Workshop on Geothermal Reservoir Engineering. Thirty-Fifth Workshop on Geothermal Reservoir Engineering. 2010, pp. 408–417.

[51] D'Amore F., and Panichi C., Evaluation of deep temperatures of hydrothermal systems by a new gas geothermometer. Geochimica et Cosmochimica Acta. Vol. 44, Issue 3. 1980, pp. 549–556.

[52] Arnórsson S., and Gunnlaugsson E., New gas geothermometers for geothermal exploration—calibration and application. Geochimica et Cosmochimica Acta. Vol. 49, Issue 6. 1985, pp. 1307–1325.

[53] Skoog D. A., Fundamentals of analytical chemistry. Thomson, 2004, 2004, p.

[54] Joseph E. P., Fournier N., Lindsay J. M., and Fischer T. P., Gas and water geochemistry of geothermal systems in Dominica, Lesser Antilles island arc. Journal of volcanology and geothermal research. Vol. 206, Issue 1–2. 2011, pp. 1–14.

[55] Delmelle P., and Bernard A., Downstream composition changes of acidic volcanic waters discharged into the Banyupahit stream, Ijen caldera, Indonesia. Journal of Volcanology and Geothermal Research. Vol. 97, Issue 1–4. 2000, pp. 55–75.

[56] Simmons S. F., and Browne P. R. L., Hydrothermal minerals and precious metals in the Broadlands-Ohaaki geothermal system: Implications for understanding low-sulfidation epithermal environments. Economic Geology. Vol. 95, Issue 5. 2000, pp. 971–999.

[57] Phuong N. K., Harijoko A., Itoi R., and Unoki Y., Water geochemistry and soil gas survey at Ungaran geothermal field, central Java, Indonesia. Journal of Volcanology and Geothermal Research. Vol. 229. 2012, pp. 23–33.

[58] Giggenbach W. F., Gonfiantini R., Jangi B. L., and Truesdell A. H., Isotopic and chemical composition of Parbati valley geothermal discharges, north-west Himalaya, India. Geothermics. Vol. 12, Issue 2–3. 1983, pp. 199–222.

[59] Delmelle P., Bernard A., Kusakabe M., Fischer T. P., and Takano B., Geochemistry of the magmatic–hydrothermal system of Kawah Ijen volcano, East Java, Indonesia. Journal of Volcanology and Geothermal research. Vol. 97, Issue 1–4. 2000, pp. 31–53.

[60] Nicholson K., Geothermal Fluids. Berlin, Heidelberg: Springer Berlin Heidelberg, 1993, 1993, p.

[61] Ii H., Geothermal and Hot Spring Water Origin Determination Using Oxygen and Hydrogen Stable Isotope in the Toyohirakawa Catchment, Hokkaido, Japan. International Journal of GEOMATE. Vol. 13, Issue 37. 2017, pp. 127–132. doi: 10.21660/2017.37.2625.

[62] Taran Y. A., Deuterium and oxygen-18 in fumarolic steam and amphiboles from some Kamchatka volcanoes:" andesitic waters", in Dokl. Akad. Nauk. USSR, 1989, Vol. 340, 1989, pp. 440–443.